Accurate, Real-Time Localization of Subminiature Inductive Transponders: Tumor Localization as an Example

Mike Beigel [*] John McGary [**]

Abstract **– We present the theoretical foundation for designing an accurate real-time, 3-D, localization system within a measurement volume. As an example, we investigate localizing a tumor during radiotherapy treatment as a challenging medical application due to the physical constraints imposed by the system. We demonstrate that real-time, three-dimensional localization of an inductive tag in the body can be accomplished with a passively charged, radio frequency transmitter and superconducting quantum interference device (SQUID) magnetometers. The overall system design consists of (1) external dipole antennas, (2) a microchip implant transmitter, and (3) SQUID magnetometers for signal detection. The transmitter is charged from external antennas where the implant IC control circuit sequentially charges and discharges. The resulting implant discharge current creates an alternating magnetic field through the inductor and is detected by a configuration of surrounding magnetometers which is then used to calculate the location of the implant transmitter. From the analysis, real-time, 3-D positioning is shown to be feasible for time scales on the order of 1 second.**

1 INTRODUCTION

Finding the exact position and orientation of a tag in a 3-D space within an energizing field is useful in a variety of applications. An example of this problem is to localize a prostate tumor in three dimensions during external beam radiotherapy and irradiate the tumor as a moving target. The radiotherapy goal is to reduce the dose to the surrounding tissue (decrease complications) and escalate the tumor radiation dose to eliminate all cancer cells. With respect to increased tumor control, localization is the decisive factor. The previous and current research efforts toward tumor localization have been, and are, limited to medical imaging modalities using ultrasound, visible light, and x-rays. With years of research toward imaging localization, these methods are currently unable to accurately determine the real-time tumor position in three dimensions. Therefore, a different approach is needed.

We propose to use a sub-miniature inductive transponder to localize a physical point in a human body for a worst case scenario involving a medical treatment procedure. Radiotherapy treatment presents a number of environmental complications that include radio frequency noise, as a result of klystrons and linear accelerator components, and radiation damage. To deal with this environment and measurement constraints, an alternating magnetic field has been selected as the signal for detection. The tag architecture proposed most closely resembles conventional RFID HDX architecture, for optimizing signal-to-noise ratio, and the energizing field would be produced by coils similar to inductive RFID antennas. To attain the necessary position accuracy, the application of SQUID magnetometers resolves position uncertainty and signal sensitivity.

With the concepts presented here, the feasibility of designing a transmitter system in terms of signal strength and real-time capability are examined. Signal generation, in terms of mode, strength, and detection are the focus of this discussion.

2 METHODS AND MATERIALS

We have chosen the magnetic induction vector as the principle source due to several design constraints illustrated in the following section. Within the category of generating and detecting a magnetic field, the time variation of the field strength can be static or dynamic. To examine a simple case of using a static field, a small magnetized bar magnet could be implanted in the desired location where the associated magnetic field strength could be used to determine the location. The physical properties associated with generating and detecting the field strength are the detector sensitivity, the magnetic field strength, and the implant size. With respect to implant size, the size should be comparable to brachytherapy seed implants that are used routinely. Therefore, an estimate for the size of the magnet or transponder dimensions is on the order of 5 mm diameter x 5 mm length. Considering these dimensions, the magnetic dipole moment, for a permanent magnet, is easily calculated using

$$M = \frac{B_i V}{\mu_0} \qquad (1)$$

where M is the magnetic dipole moment (A-m^2), B_i is the intrinsic magnetic induction of the permanent

[*] Mike Beigel, CEO, Beigel Technology Corp., Encinitas, California USA http://www.beigeltech.com, {mike@beigeltech.com}
[**] Prof. John McGary, Baylor College of Medicine, Houston, Texas USA {jcmcgary@bcm.edu}

magnet (Tesla), V is the volume (m^3), and μ_0 is the permeability constant = $4\pi 10^{-7}$ H/m. Using typical values for the magnetic induction, B_i, ~.5 T for ceramic or ferrite magnets, and the magnet dimensions, V=1.25 10^{-7} m^3, M is approximately 0.05 A-m^2. With these values, the magnitude of the magnetic induction field at large distances, along the direction of the magnetic moment, is calculated using the magnetic dipole equation:

$$B \approx \frac{\mu_0 \cdot M}{4\pi r^3} \qquad (2)$$

where the approximation is used for distances much larger than the permanent magnet dimensions.

At a distance of 1 m from the permanent magnet, B ~ 5 nT which can be measured using conventional magnetometers in magnetic quiet environments. However, if implant position accuracy is to be resolved within 2 mm, the detectors will be required to measure induction signals in the range of pT which is insufficient for detection using conventional magnetometers except in magnetically shielded rooms.

The variation of B(r) as a function of distance between the point of measurement and the magnet is dB(r) ~ (-3 B(r)/r) dr. As the detection distance from the magnet decreases, the magnetic induction increases by r^3 that reduces the sensitivity needed for the detectors, however, dB(r) continues to be relatively small even at a distance of 50 cm which is important for clinical applications.

Acknowledging that the magnetic flux density from a permanent magnet is relatively small compared with the radio frequency noise generated from linear accelerator components, another method for generating a magnetic field is needed. Pulsing the induction field will allow detectors to discriminate the desired signal from other static and oscillating magnetic fields within the treatment room. With a defined generating frequency, the associated detectors can selectively filter out the background fields and measure the comparatively small magnetic signal field strength.

For conditions where the frequency is zero, the magnetic field intensity reduces to the static dipole equation:

$$H = \left(\frac{m_0}{4\pi r^3}\right)\left[2\cos\theta\,\hat{r} + \sin\theta\,\hat{\theta}\right] \qquad (3).$$

There are a number of factors to consider with regard to this type of design using an oscillating magnetic dipole to generate a detection signal, mainly (1) the operating frequency, (2) detector distance, (3) energy source, and (4) size of the device. Each of these factors are mutually dependent and require a balance to meet the basic design constraints. This is known as the far field region and Equation 3 is applied in that region. The transition reference distance between the far and near field is described by RF=$\lambda/2\pi$. For low frequency operation, near 100 kHz, the transition distance is about 350 m which is well within the typical medical environment distance constraints.

Within the far field region, the electromagnetic energy dissipation is a function of frequency. The energy density for conductors is described by

$$S_{avg} = .5\sqrt{\left(\frac{\sigma}{2\omega\mu}\right)}\exp(-2z/\delta)\cdot E_0^2 \qquad (4)$$

where z is the propagation distance, δ is the skin depth, ω is the angular frequency, σ is the conductivity, μ is the permeability of the medium. Dissipation within a conducting medium is dependent upon the square root of the frequency$\sqrt{}$ f) – higher frequencies are attenuated more than lower frequencies. For tissue, the energy attenuation is approximately –7.96 dB/10 cm at 10 MHz and decreases to approximately -.252 dB/10 cm at 1 KHz.[3]

In contrast, if the operating frequency is within the low frequency range, 50 – 200 kHz, attenuation problems are essentially eliminated and Equation 3 can be used. This reduces the complexity of the problem; induction becomes the major model and simple circuits can be used for the overall system design. Figure 1 represents the basic electronic circuit for passive charging where charge can be accumulated using rectifiers in several ways. The transponder is linked to the external dipole antenna by induction. Providing power to the transponder by the partial flux depends upon the relative geometry and position of the two conductor loops. Charge can be accumulated over time (sequential) or during operation (duplex).

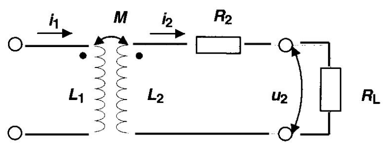

Figure 1. Near field approximation reduces to circuit.

Higher antenna frequencies generate more induction current and load voltage but are also attenuated more through tissue. Hence, the operating frequency requires some degree of optimization and operating at the resonant frequency of the parallel resonant circuit can reduce some losses. The step up voltage is difficult to calculate due to the mutual inductance dependence on geometry. Distance and modeling/empirical data will be required for design details. In the implant tag circuit, the load resistance can be switched at a threshold voltage such that the internal resistance falls abruptly when the threshold is exceeded. In this configuration, power can be transmitted continuously to the implant signal generating circuit without interruption as long as the mutual inductance, frequency, and operating voltage are matched.

3 RESULTS

Power to the transmitter is transferred using a large inductor coil with an alternating magnetic field placed within the range of the implant coil. There are several points to consider for this type of configuration design: (1) the minimum magnetic field strength as a function of distance required to power the implant circuit, (2) the inductor coil loop radius, (3) the operating frequency, and (4) the associated licensing regulations governing electromagnetic emissions.

To estimate some of the properties associated with the power antenna design, equation 3 can be used to calculate the magnetic field intensity along the magnetic moment axis of the coil where R is the radius of the antenna coil and x is the distance along the normal axis to the coil plane. Solution to the equation indicates that the maximum intensity is generated with an antenna radius ~ R√2. For practical design estimates, the field intensity can be considered to have a maximum value at distances that are approximately equal to the antenna radius.

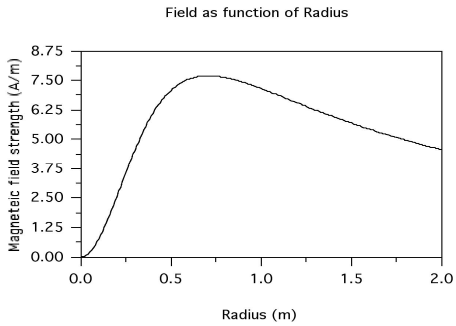

Figure 2. H(x=0.5m, R). The field intensity at x=0.5 m as a function of antenna radius (R).

Furthermore, these simple calculations demonstrate that the field strength is relatively flat for distances less than the antenna coil radius (x<R) and then decrease sharply for distances larger than the radius. Although not shown here, the dipole antenna magnetic field intensity decreases rapidly in the near field region, 60 dB per decade, and then decreases more slowly in the far field region, 20 dB per decade. Therefore, the dipole radius should be as large as possible and the tag should be located within a distance comparable to the antenna radius.

With respect to the implant circuit, it is useful to estimate the minimum magnetic field intensity that is just sufficient to supply enough energy to operate the additional support circuitry (full duplex mode) at the maximum distance from the implant. Using the basic circuit, the voltage drop across the load resistor can be calculated using

$$u_2 = \frac{j\omega\mu_0 H_{eff} AN}{1 + (j\omega L_2 + R_2)(\frac{1}{R_L} + j\omega C_2)} \qquad (5)$$

where H_{eff} is set to H_{min}. Figure 3 shows that the minimum field strength corresponds to the resonant frequency of the LC implant circuit. In Figure 3, we have selected reasonable approximations for the implant device for the expected operating conditions: N_2=10, L_2=10^{-5} H, C_2=10^{-5} F, R_2=10^{3} Ω, R_L=10, Ωcoil radius =.002 m, u_2=.01 V, and μ_r=2500. However, for illustration, we chose an operating potential for the circuit as 10 mV that is far too small for practical chip design. Without substantial improvements in the circuit parameters such as the permeability of the inductor core or loop radius, the magnetic field strength will be larger than allowable which demonstrates the difficulty in designing a full or half duplex circuit of these dimensions.

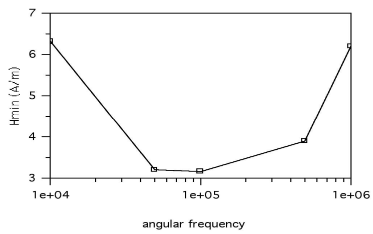

Figure 3. Minimum field strength to power tag.

However, if the field strength is insufficient to power the tag, then a sequential mode can be implemented. Again, operating in the near field reduces the complexity of the problem and the circuit analysis can be used to model the system. With that assumption, the equation describing the system is well known and can be solved easily using:

$$L_2 \cdot \frac{d^2 Q_2(t)}{dt^2} + R_2 \cdot \frac{d\, Q_2(t)}{dt} + \frac{Q_2(t)}{C_2} = M_{12} \frac{dI_1(t)}{dt} \qquad (6),$$

where the mutual inductance is the primary unknown but can be approximated. The magnetic field strength can then be computed with reasonable values assumed for the circuit as shown in Figure 4.

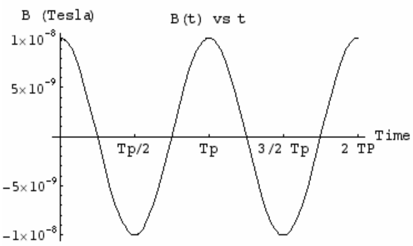

Figure 4. Steady state solution showing signal strength at detector.

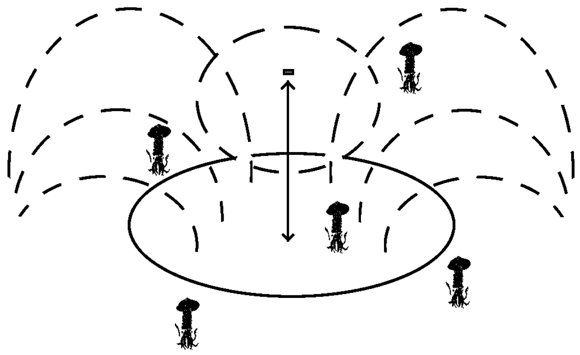

Figure 5. Example of energizing dipole loop and field lines, measurement volume, inductive tag, and multiple SQUID sensors.

4 DISCUSSION

Since the duplex mode will not work using the design constraints defined for this problem, the sequential mode is used. Further analysis shows that the sequential mode is able to charge and discharge within 1 second and create field strengths at 1 meter that can be detected with SQUID magnetometers. These values are based upon simple models for the mutual inductance and not based on detailed real time motion. To increase the mutual inductance, several dipole antennas can be placed at different angles to account for the relative geometry and continually charge the tag circuit regardless of the how the tag is implanted or oriented during treatment. The additional advantage of operating in a sequential mode is that the charge can be integrated before treatment and then cycled during treatment at different rates and currents. This increases flexibility in real-time constraints and detector distances as well as simplifying the design. An example design with all essential electromagnetic components is shown in Figure 5.

5 CONCLUSION

We have demonstrated the feasibility of using a passive, inductively coupled transmitter as a source for real-time, 3-D localization. The overall system consists of multiple dipole antennas to power the tag and SQUID magnetometers for signal detection. The analysis demonstrates that the device is required to operate at low frequencies and charge through a sequential mode due to the low mutual inductance and tag inductor size. With realistic approximations for the mutual inductance, detectable signals at 1 meter can be created within 1 second. To increase the mutual inductance, multiple antennas can be configured to decrease charge times and increase field strengths. In addition, the sequential operating mode allows for pre-treatment charging to provide greater signal strengths and faster real-time position updates.

These methods can easily be extended to other medical applications and general applications where accurate localization is needed within a defined volume.

References

[1] M. Beigel, "Dynamic Performance of Inductive RFID Systems", Proceedings of ECCTD '99, Vol. 1, pp. 29-33. http://www.beigeltech.com/articles/dynamic1.html

[2] J. Mc Gary, "Theoretical foundation for real-time prostate localization using an inductively coupled transmitter and a superconducting quantum interference device (SQUID) magnetometer system", J. App. Clin. Med. Phys, 5 (4), 29-45, 2004.

[3] Lo YT, Lee SW. Antenna handbook, vol. III. Kluwer Academic Publishers; 1993.

[4] Schuermann, J., Meier, H., TIRIS – Leader in radio frequency identification technology, Texas Instruments Technical Journal, TITJ Vol. 10, No. 6, Nov. 1993, pp. 2-14

[5] K. Finkenzeller, RFID HANDBOOK Second Edition, 2002, ISBN 0-470-84402-7, Chapter 2, 3, 4